PHYSICAL REVIEW A **70**, 012312 (2004)

Scaling of multiple postselected quantum gates in optics

T. C. Ralph
Centre for Quantum Computer Technology, Department of Physics, University of Queensland, St. Lucia 4072, Australia
(Received 8 April 2004; published 27 July 2004)

We show that interesting multigate circuits can be constructed using a postselected controlled-sign gate that works with a probability $(1/3)^n$, where $n-1$ is the number of controlled-sign gates in the circuit, rather than $(1/9)^{n-1}$, as would be expected from a sequence of such gates. We suggest some quantum information tasks which could be demonstrated using these circuits, such as parity checking and cluster-state computation.

DOI: 10.1103/PhysRevA.70.012312 PACS number(s): 03.67.−a, 42.50.−p, 42.50.Xa

I. INTRODUCTION

The techniques of linear optical quantum computation (LOQC) [1] can be used to implement nontrivial two-qubit gates, nondeterministically, with linear optics and photon detection. In principle these gates can be made heralded, however, the efficiency requirements on photon production and detection to achieve this cannot presently be met [2]. Once heralded gates are achieved (and assuming high efficiency photon storage) a number of schemes for achieving deterministic or near-deterministic operation have been proposed [1,3,4]. In the interim there is considerable interest in the construction of small scale circuits that can test the basic principles of LOQC with reasonable success probabilities. With this in mind, it is important to identify the most efficient ways to construct said circuits.

Thus far there have been two demonstrations of controlled-not (CNOT), or equivalently controlled-sign (CS) gates using LOQC [5,6], both of which rely on postselection via coincidence detection. The simpler of these [6] does not require any auxiliary photon inputs and works with a probability of 1/9 [7]. As a result this gate, which we will refer to as a two-photon CS, is a good candidate for use in small quantum circuits [8,9]. However, a success rate of 1/9 rapidly becomes impractical when a few gates are needed, and a better scaling would be a major advantage. In this paper we describe a way of concatenating such gates so that a significant scaling advantage is obtained. In the next section we will describe the basic arrangements and the equivalent quantum circuits. In Sec. III we will discuss some useful circuits which can be built from these building blocks. We conclude with Sec. IV.

II. MULTIPLE GATES

The key observation of this paper is that the sequence of CS gates shown in Fig. 1 can be implemented, up to local unitaries, in the coincidence basis, by a single optical circuit. The probability of success of this circuit scales as $(1/3)^n$, where n is the number of qubits in the circuit, rather than the $(1/9)^{n-1}$ scaling which would occur if the circuit was constructed from a sequence of two-photon CS gates.

To show this we consider constructing the gate piece by piece. The primary element is the basic two-photon CS gate [7,10] shown in Fig. 2(a). Here the qubits are encoded as shown as the presence in one of two modes of a single photon (dual rail logic). Thus a logical zero is $|0\rangle_L = |01\rangle$, where $|ij\rangle$ is a two-mode state in which i is the occupation of the upper mode [in Fig. 2(a)] and j is the occupation of the lower mode. Similarly $|1\rangle_L = |10\rangle$. The circuit produces the following transformation on an arbitrary two-qubit input state:

$$\alpha_1|01\rangle|01\rangle + \alpha_2|01\rangle|10\rangle + \alpha_3|10\rangle|01\rangle + \alpha_4|10\rangle|10\rangle \rightarrow \frac{1}{3}(\alpha_1|01\rangle|01\rangle + \alpha_2|01\rangle|10\rangle - \alpha_3|10\rangle|01\rangle + \alpha_4|10\rangle|10\rangle), \tag{1}$$

provided a single photon is found in each of the output qubits (i.e., we reject events where one or more of the output qubits does not contain a photon). We see that the action of the circuit is to perform a CS gate in which the flipped element is $|1\rangle_L|0\rangle_L$. This is represented graphically in Fig. 2(b) with a solid dot representing the qubit that should be "1" and an open dot representing the qubit that should be "0" for the flip to occur. The probability that the gate will succeed is 1/9. This gate was demonstrated in [6].

We now consider adding another qubit to the circuit as shown in Fig. 3(a). The circuit now produces the following transformation on an arbitrary three-qubit input state:

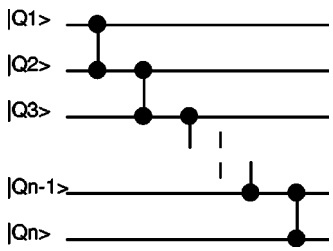

FIG. 1. Quantum circuit consisting of n qubits in which all nearest neighbors are linked by CS gates. In line with the normal definition of CS gates, the solid balls indicate that the flipped component is the $|1,1\rangle_L$ element.

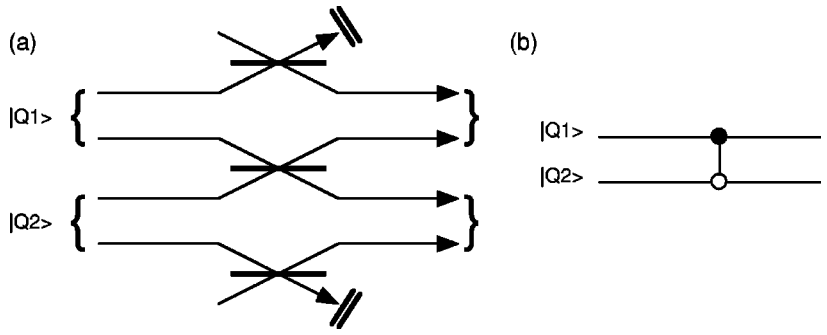

FIG. 2. (a) Optical circuit for the basic CS gate. All beam splitters have a reflectivity of $1/3$ and we adopt the convention that reflection off the top of a beam splitter results in a π phase shift. The unlabeled inputs represent vacuum modes. (b) Equivalent qubit circuit where the solid upper ball and open lower ball on the CS gate indicates that the flipped component is the $|1,0\rangle_L$ element.

$$\alpha_1|01\rangle|01\rangle|01\rangle + \alpha_2|01\rangle|10\rangle|01\rangle + \alpha_3|10\rangle|01\rangle|01\rangle + \alpha_4|10\rangle|10\rangle|01\rangle + \alpha_5|01\rangle|01\rangle|10\rangle + \alpha_6|01\rangle|10\rangle|10\rangle + \alpha_7|10\rangle|01\rangle|10\rangle + \alpha_8|10\rangle|10\rangle|10\rangle \rightarrow \frac{1}{\sqrt{27}}(-\alpha_1|01\rangle|01\rangle|01\rangle - \alpha_2|01\rangle|10\rangle|01\rangle + \alpha_3|10\rangle|01\rangle|01\rangle - \alpha_4|10\rangle|10\rangle|01\rangle - \alpha_5|01\rangle|01\rangle|10\rangle + \alpha_6|01\rangle|10\rangle|10\rangle + \alpha_7|10\rangle|01\rangle|10\rangle + \alpha_8|10\rangle|10\rangle|10\rangle). \quad (2)$$

It is straightforward to show that this transformation is equivalent to the quantum circuit shown in Fig. 3(b). Notice that the probability of success is $1/27$, which should be compared with a probability of success of $1/9^2=1/81$, which would be achieved if two of the gates of Fig. 2(a) were placed in succession.

Finally, to make the trend clear, we consider adding another qubit to the gate as shown in Fig. 4(a). The circuit now produces the following transformation on an arbitrary four-qubit input state:

$$\alpha_1|01\rangle|01\rangle|01\rangle|01\rangle + \alpha_2|01\rangle|10\rangle|01\rangle|01\rangle + \alpha_3|10\rangle|01\rangle|01\rangle|01\rangle + \alpha_4|10\rangle|10\rangle|01\rangle|01\rangle + \alpha_5|01\rangle|01\rangle|10\rangle|01\rangle + \alpha_6|01\rangle|10\rangle|10\rangle|01\rangle + \alpha_7|10\rangle|01\rangle|10\rangle|01\rangle + \alpha_8|10\rangle|10\rangle|10\rangle|01\rangle + \alpha_9|01\rangle|01\rangle|01\rangle|10\rangle + \alpha_{10}|01\rangle|10\rangle|01\rangle|10\rangle + \alpha_{11}||10\rangle|01\rangle|01\rangle|10\rangle + \alpha_{12}|10\rangle|10\rangle|01\rangle|10\rangle + \alpha_{13}|01\rangle|01|10\rangle|10\rangle + \alpha_{14}|01\rangle|10\rangle|10\rangle|10\rangle + \alpha_{15}|10\rangle|01\rangle|10\rangle|10\rangle + \alpha_{16}|10\rangle|10\rangle|10\rangle|10\rangle \rightarrow \frac{1}{\sqrt{81}}(\alpha_1|01\rangle|01\rangle|01\rangle|01\rangle + \alpha_2|01\rangle|10\rangle|01\rangle|01\rangle - \alpha_3|10\rangle|01\rangle|01\rangle|01\rangle + \alpha_4|10\rangle|10\rangle|01\rangle|01\rangle + \alpha_5|01\rangle|01\rangle|10\rangle|01\rangle - \alpha_6|01\rangle|10\rangle|10\rangle|01\rangle - \alpha_7|10\rangle|01\rangle|10\rangle|01\rangle - \alpha_8|10\rangle|10\rangle|10\rangle|01\rangle + \alpha_9|01\rangle|01\rangle|01\rangle|10\rangle + \alpha_{10}|01\rangle|10\rangle|01\rangle|10\rangle - \alpha_{11}|10\rangle|01\rangle|01\rangle|10\rangle + \alpha_{12}|10\rangle|10\rangle|01\rangle|10\rangle - \alpha_{13}|01\rangle|01\rangle|10\rangle|10\rangle + \alpha_{14}|01\rangle|10\rangle|10\rangle|10\rangle + \alpha_{15}|10\rangle|01\rangle|10\rangle|10\rangle + \alpha_{16}|10\rangle|10\rangle|10\rangle|10\rangle). \quad (3)$$

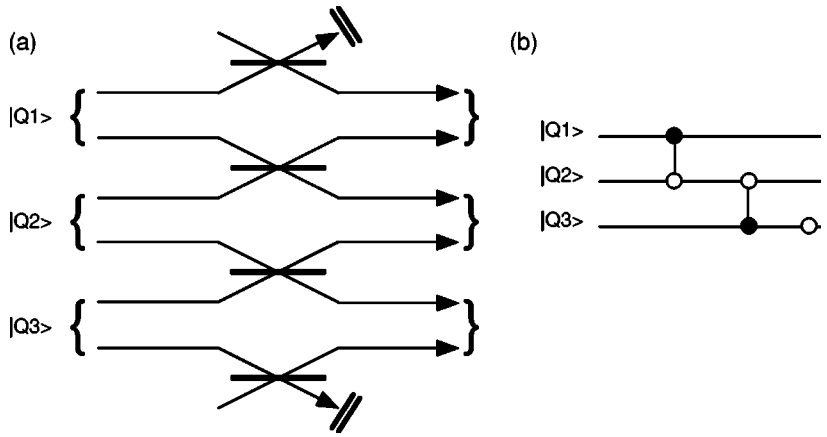

FIG. 3. (a) Optical circuit for two cascaded CS gates. All beam splitters have a reflectivity of $1/3$ and we adopt the convention that reflection off the top of a beam splitter results in a π phase shift. The unlabeled inputs represent vacuum modes. (b) Equivalent qubit circuit where the solid upper ball and open lower ball on the first CS gate indicates that the flipped component is the $|1,0\rangle_L$ element, while the inverse on the second CS gates indicates that the flipped component is the $|0,1\rangle_L$ element. The open circle indicates a sign flip on the zeroth element of the indicated qubit.

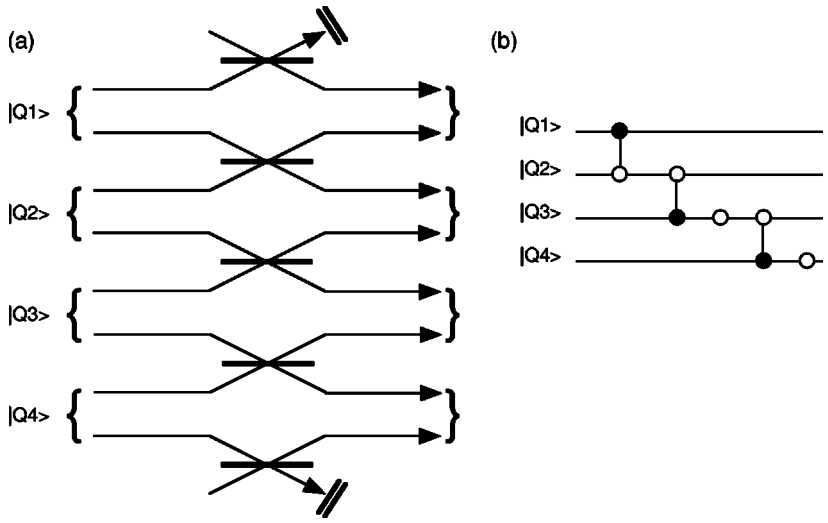

FIG. 4. (a) Optical circuit for three cascaded CS gates. All beam splitters have a reflectivity of $1/3$ and we adopt the convention that reflection off the top of a beam splitter results in a π phase shift. The unlabeled inputs represent vacuum modes. (b) Equivalent qubit circuit where the solid upper ball and open lower ball on the first CS gate indicates that the flipped component is the $|1,0\rangle_L$ element, while the inverse on the second and third CS gates indicates that the flipped component is the $|0,1\rangle_L$ element. The open circles indicate sign flips on the zeroth elements of the indicated qubits.

Again, it is straightforward (if not somewhat tedious) to show that this transformation is equivalent to the quantum circuit shown in Fig. 4(b). The trend is now clear: adding an extra qubit to the optical circuit links an additional qubit to the quantum circuit via a controlled-sign operation with a local sign change also applied. This produces a circuit that is locally equivalent to the circuit of Fig. 1. The probability of success scales as $(1/3)^n$, where n is the number of qubits, as claimed earlier. In the next section we consider some interesting demonstration circuits that can be built using this technique.

III. CIRCUITS

Although the optical arrangements discussed in the previous section produce only specific circuits, these are quite useful circuits. We briefly discuss some quantum information tasks that could be demonstrated using the basic arrangement of the previous section. (Note that, of course, all these circuits only work nondeterministically and only in the coincidence basis.)

GHZ production and detection. The circuit depicted in Fig. 5 will produce all eight maximally entangled three-particle Greenberger, Horne, and Zeilinger (GHZ) states [11] as a function of the eight possible computational state arrangements at the input. For example, if the computational state $|1\rangle_L|1\rangle_L|1\rangle_L$ is sent into the circuit the GHZ state $|1\rangle_L|1\rangle_L|0\rangle_L-|0\rangle_L|0\rangle_L|1\rangle_L$ is produced. The probability of success is $1/27$. Just as interestingly, if run in reverse, this circuit can distinguish all eight GHZ states by disentangling

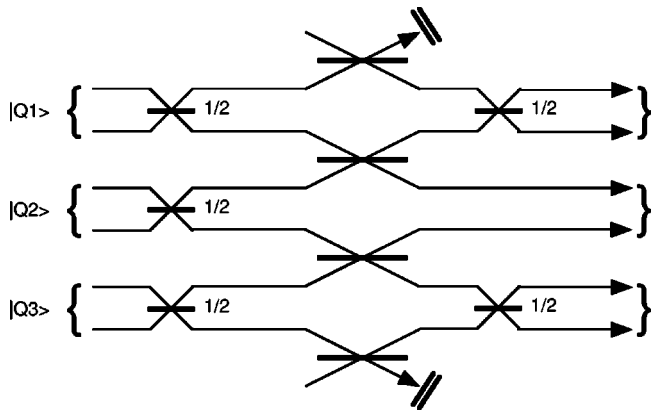

FIG. 5. Optical circuit for producing GHZ states. All beam splitters have a reflectivity of $1/3$, except those labeled "$1/2$." We adopt the convention that reflection off the top of a beam splitter results in a π phase shift. The unlabeled inputs represent vacuum modes.

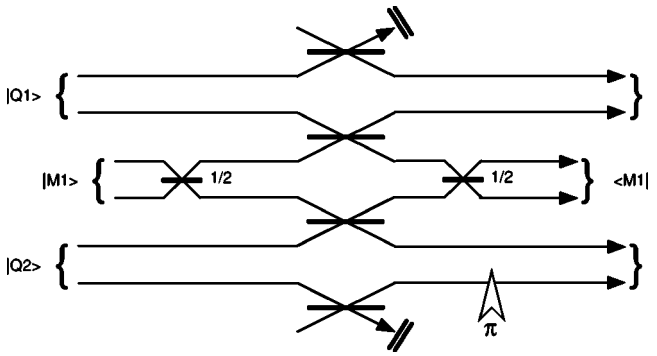

FIG. 6. Optical circuit for demonstrating parity checking. The ancilla qubit $|M1\rangle$ is prepared in the $|1\rangle_L$ state. If the qubits ($|Q1\rangle$ and $|Q2\rangle$) are in an even-parity state the ancilla qubit will not be flipped. If the qubits are in an odd-parity state the ancilla qubit will be flipped. "π" indicates a π phase shift. All beam splitters have a reflectivity of $1/3$, except those labeled "$1/2$." We adopt the convention that reflection off the top of a beam splitter results in a π phase shift. The unlabeled inputs represent vacuum modes.

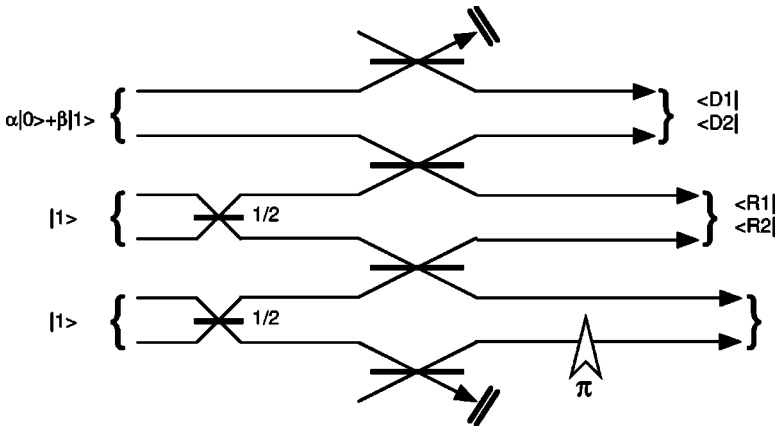

FIG. 7. Optical circuit for demonstrating a simple cluster state (see text for description). "π" indicates a π phase shift. All beam splitters have a reflectivity of $1/3$, except those labeled "$1/2$." We adopt the convention that reflection off the top of a beam splitter results in a π phase shift. The unlabeled inputs represent vacuum modes.

them into the eight orthogonal computational qubit arrangements.

Parity checking. The circuit depicted in Fig. 6 can measure the parity of a two-qubit state of definite parity nondestructively. An even-parity state will not flip the value of the ancilla qubit, while an odd-parity state will. This can be used to demonstrate a simple form of bit-flip error correction [9]. For example, suppose we prepare the even-parity state $\alpha|0,0\rangle_L+\beta|1,1\rangle_L$. If a bit-flip error occurs on one of the qubits then the state will become odd parity. The parity checking circuit will thus identify if a bit-flip has occurred. Regardless of the outcome of the parity measurement the superposition is preserved.

Cluster states. Recently, Raussendorf and Briegel have suggested a cluster-state model for quantum computation [12]. Nielsen has suggested that LOQC quantum computation is more easily implemented based on this model [4]. Any evolution of a single qubit can be simulated by: (i) preparing a string of qubits all in the states $|0\rangle_L+|1\rangle_L$, (ii) linking each nearest neighbor by CS gates, and then (iii) measuring the single qubits in the string in sequence. The measurement basis chosen for each qubit depends on the single qubit unitaries one wishes to simulate and the result of the measurement of the preceding qubit. Each qubit measurement simulates the unitary evolution $\hat{H}\hat{R}(Z,\theta)$, where $\hat{H}$ is the Hadamard transformation defined by $\hat{H}|0\rangle\rightarrow|0\rangle+|1\rangle, \hat{H}|1\rangle\rightarrow|0\rangle-|1\rangle$, and $\hat{R}(Z,\theta)$ is a z rotation defined by $\hat{R}(Z,\theta)|0\rangle\rightarrow|0\rangle$, $\hat{R}(Z,\theta)|1\rangle\rightarrow e^{i\theta}|1\rangle$. An arbitrary single qubit unitary can be simulated using a four-qubit cluster state and three measurements.

Figure 7 depicts how a single qubit cluster-state evolution might be demonstrated. For simplicity we consider the arbitrary x rotation, $\hat{R}(X,\theta)=\hat{H}\hat{R}(Z,\theta)\hat{H}$, which can be achieved with a three-qubit cluster state and two measurements. The top qubit is prepared in some arbitrary state. A cluster state is then formed by applying our CS circuit to the arbitrary qubit and two other qubits prepared in diagonal states. The idea is then to simulate the single qubit x rotation via measurement. The upper qubit is measured first in the diagonal basis: $|D1\rangle=|0\rangle_L+|1\rangle_L$, $|D2\rangle=-|0\rangle_L+|1\rangle_L$ [13]. If the outcome is $D1$, then the middle qubit is measured in the phase rotated basis: $|R1(\theta)\rangle=|0\rangle_L+\exp\, i\theta|1\rangle_L$, $|R2(\theta)\rangle=-|0\rangle_L+\exp\, i\theta|0\rangle_L$. If the outcome is $D2$, then the middle qubit is measured in the phase antirotated basis: $|R1(\theta)\rangle=|0\rangle_L+\exp -i\theta|1\rangle_L$, $|R2(\theta)\rangle=-|0\rangle_L+\exp -i\theta|1\rangle_L$. After these measurements the state of the lower qubit is the same as that of the original qubit, but rotated about x by an angle θ. However, the effective computational basis of the qubit depends on the outcomes of the measurements in the following way: (i) $D1, R1(\theta)$: the original computational basis. (ii) $D1, R2(\theta)$: bit flip of the original computational basis. (iii) $D2, R1(-\theta)$: phase flip of the original computational basis. (iv) $D2$, $R2(-\theta)$: bit flip and phase flip of the original computational basis.

IV. CONCLUSION

We have discussed the construction of multiqubit, multientangling gate circuits in optics. We have shown that by using a concatenated circuit, multiple two-qubit gates can be applied with improved success probability. We have shown that the resulting circuits can be used to demonstrate interesting quantum tasks, such as GHZ state production and analysis, parity checking, and simple cluster-state computation.

For clarity we have described gate construction in terms of spatially dual rail qubits however, obviously, any implementation would also exploit the polarization degree of freedom for encoding and manipulating the qubits. Indeed, because of the symmetry of the proposed gates, techniques similar to those used in Ref. [6] should be adaptable to the proposed gates.

Although, because of their nondeterministic and coincident nature the proposed gates are not scalable, the experiments suggested here can demonstrate the basic principles and should reveal much about the challenges that will be faced by the scalable gates, which will follow when technology allows. It is possible that the basic principle used here of concatenating gates to improve their performance may be applicable in other scenarios.

ACKNOWLEDGMENTS

We acknowledge useful discussions with M. Nielsen, C.C. Harb, Ch. Silberhorn, and G. Pryde. This work was supported by the Australian Research Council.

[1] E. Knill, L. Laflamme, and G. J. Milburn, Nature (London) **409**, 46 (2001).
[2] A. P. Lund, T. B. Bell, and T. C. Ralph, Phys. Rev. A **68**, 022313 (2003).
[3] N. Yoran and B. Reznik, Phys. Rev. Lett. **91**, 037903 (2003).
[4] M. A. Nielsen, e-print quant-ph/0402005 (2004).
[5] T. B. Pittman, M. J. Fitch, B. C. Jacobs, and J. D. Franson, Phys. Rev. A **68**, 032316 (2003).
[6] J. L. O'Brien, G. J. Pryde, A. G. White, T. C. Ralph, and D. Branning, Nature (London) **426**, 264 (2003).
[7] T. C. Ralph, N. K. Langford, T. B. Bell, and A. G. White, Phys. Rev. A **65**, 062324 (2002).
[8] J. L. Dodd, T. C. Ralph, and G. J. Milburn, Phys. Rev. A **68**, 042328 (2003).
[9] T. C. Ralph, IEEE J. Sel. Top. Quantum Electron. **9**, 1495 (2003).
[10] H. F. Hofmann and S. Takeuchi, Phys. Rev. A **66**, 024308 (2002).
[11] D. Greenberger, M. Horne, and A. Zeilinger, in *Bell's Theorem, Quantum Theory, and Conceptions of the Universe*, edited by M. Kaftos (Kluwer, Dordrecht, 1989).
[12] R. Raussendorf and H. J. Briegel, Phys. Rev. Lett. **86**, 5188 (2001).
[13] More generally the unitary $\hat{R}(X,\theta)\hat{R}(Z,\phi)$ can be implemented with this circuit by making the first measurement in the basis: $|D1(\phi)\rangle = |0\rangle_L + \exp\, i\phi|1\rangle_L$, $|D2(\phi)\rangle = -|0\rangle_L + \exp\, i\phi|1\rangle_L$.